Computers, Materials & Continua
DOI: 10.32604/cmc.2022.031291
Article

Tech Science Press

Outage Probability Analysis of Free Space Communication System Using Diversity Combining Techniques

Hasnain Kashif* and Muhammad Nasir Khan

Department of Electrical Engineering, The University of Lahore, Lahore, 54000, Pakistan
*Corresponding Author: Hasnain Kashif. Email: dee01153001@student.uol.edu.pk
Received: 14 April 2022; Accepted: 10 June 2022

Abstract: Recently, free space optical (FSO) communication is gaining much attention towards the research community. The reason for this attention is the promises of high data-rate, license-free deployment, and non-interfering links. It can, however, give rise to major system difficulties concerning alignment and atmospheric turbulence. FSO is the degradation in the signal quality because of atmospheric channel impairments and conditions. The worst effect is due to fog particles. Though, Radio Frequency (RF) links are able to transmit the data in foggy conditions but not in rain. To overcome these issues related to both the FSO and RF links. A free space communication system (FSCS) is proposed, in which the hybrid technology is based on the individual FSO and RF channel. FSCS is a capable solution to overcome the difficulties of the existing systems (FSO and RF) as well as to enhance the overall link reliability and availability. In this paper, FSCS is investigated in terms of performance throughput (i.e., outage probability and bit-error-rate (BER)) by implementing the receive diversity combining techniques. An analysis of the outage probability of the proposed system along with the individual FSO and RF system is developed. Simulation results are presented to support the analysis. It is shown that the proposed system outperforms the individual FSO and RF system and gives a power gain of 3dB over a distinct number of receive antennas.

Keywords: Atmospheric turbulence; free space communication system; power management; signal independent noise; line of sight

1 Introduction

In the recent era, free space optical (FSO) communication systems are taken into consideration as an auspicious answer to the numerous applications consuming high bandwidth. The primary benefits of FSO include high-capacity and unlicensed spectrum. Owing to the provision of a huge variety of broadband, systems 5 with low priced implementation and less power consumption are preferred. Presently, the trade-off is twofold but the unknown channel conditions and crucial pointing issues, make optical systems less stable than the conventional radio-frequency (RF) communication systems [1,2]. The FSO system implementation has some crucial difficulties including-atmospheric turbulence, degradation in link quality and Line of sight (LOS) [3]. Along with the inherited benefits of the optical spectrum though it suffers from various drawbacks when 10 utilizing it over a long distance employing the multiplexing techniques. These drawbacks include modal dispersion, linear coupling (referred to as cross-talk), and non-linear effects [4]. Due to the presence of these drawbacks, the optical received signal gets and is attenuated by turbulence, mis-alignment and divergence. To overcome these issues, various techniques have been presented in [5–9]. The most prominent are the accurate pointing, acquisition and tracking, digital signal processing, adaptive optics and modifying transmitted beams are employed, which support minimizing the effect of modal coupling and cross-talk. Even in the era of machine learning, neural network models are also recommended to limit such drawbacks of optical channel transmission [10,11]. Much research works on wireless sensor networks, which have limited energy and transmission capacity [12–20].

To further improve the capacity of the optical channel, it is recommended to employ an optical system carrying multiple optical beams and exploit the multiplexing technique i.e., mode division multiplexing (MDM), orbital-angular-momentum (OAM) multiplexing [21–25]. Implementing the MDM along with the OAM multiplexing, immensely raises the channel capacity of the optical links adding more difficulty for the eavesdropper. Also, Luminescent solar concentrators are suggested to improve the optical gain in case of visible light communications. A complete list of acronyms and symbols is provided in Tabs. 1 and 2 respectively.

Table 1: List of acronyms

Acronyms	Abbreviations
BPSK	Binary phase shift keying
BER	Bit error rate
CDF	Cumulative density function
DEC	Decoder
ENC	Encoder
EGC	Equal gain combiner
E/O	Electrical to optical
FSO	Free space optical
FSCS	Free space communication system
GGD	Gamma-Gamma distribution
GBps	Giga-bit per second
IM/DD	Intensity modulation with direct detection
LDPC	Low density parity check
LED	Light emitting diodes
LOS	Line of sight
MISO	Multiple input single output
MIMO	Multiple input multiple output
MDM	Mode division multiplexing
OAM	Orbital-angular-momentum
OOK	On-off keying

(Continued)

Table 1: Continued

Acronyms	Abbreviations
PIN	Positive-intrinsic-negative
PDF	Probability density function
RF	Radio frequency
SNR	Signal-to-noise ratio
SD	Spatial diversity
SIMO	Single input multiple output
SC	Selection combiner
MRC	Maximum ratio combiner
VLC	Visible light communication
5G	5th generation

Table 2: List of symbols

Symbols	Parameter	Symbols	Parameter
k	Information bits	n	Encoded bits
n_r	Encoded bits over the RF channel	n_o	Encoded bits over the FSO channel
$\mathcal{X}$	FSO channel input constellations	$\hat{\mathcal{X}}$	RF channel input constellations
$\hat{x}$	RF channel symbols	x	FSO channel symbols
γ_{FSO}	Optical channel SNR	γ_{RF}	RF channel SNR
α, η	Optical channel parameters	R_p	Detector conversion efficiency
$\hat{P}$	RF power	P	Optical power
$\hat{h}$	RF channel fading	h	Optical channel fading
D	Receive aperture diameter	L	Link distance
θ	Divergence transmit beam	α_o	Climate attenuation coefficient

Overall performance degrading components in the FSO systems because mainly at large distances are the induced fading of disturbances or turbulence occurrences [26]. For the FSO systems, typical decay can last milliseconds and it operates at the rate of several gigabits per seconds (GBps). As a result, a single fade can bring about the lack of a massive variety of serial bits. Researchers investigating the diversity techniques such as channel coding [27], advanced sequence detection techniques [28] and spatial diversity [29–32] to 30 overcome the difficulties of the FSO systems. The spatial diversity (SD) is most prominent due to the lower computational complexity. The main purpose is to reduce the computational complexity by using the combining techniques. Multiple transmission and reception patterns are exploited to employ the diversity combining techniques, which are well established in the RF communication systems. The same can be done in FSO systems and the detailed investigation to be carried out. In [30,31], authors have presented the outage probability analysis over the coherent FSO system by employing the receive diversity schemes. The focus was on the spatial selectivity of associative receptors that minimize the effect of background irradiation.

Diversity combining technique is broadly applicable to enhance the overall performance of wireless communication systems [29–31]. The diversity technique is suggested for mitigating the fading induced by the atmospheric turbulence [33,34]. Mostly the three types of spatial diversity, which are single input multiple outputs (SIMO), multiple inputs single output (MISO) and multiple inputs multiple outputs (MIMO) have been investigated [35,36] Diversity combining technique using multiple lasers and apertures to mitigate the fading effects is presented in [36]. Diversity combing can be implemented either on the transmitter or the receiver side. The receive diversity is more practical in mobile communication systems, since the transmitter has several limitations such as it cannot deserve considerable power consumption and processing complexity. Receive diversity combining technique collects numerous copies of the transmitted signal at the receiver, which are encountered by the distinct fading channels. The cumulative copies of the received signal are exploited to retrieve the transmitted signal [37]. The well-known combiners are the selection combiner (SC), maximum ratio combiner (MRC) and equal gain combiner (EGC) [38].

Researchers are developing a major communication technology by investigating the exploitation of radio links to compensate for system instability and name it a hybrid FSO-RF link. The research community started working on the hybrid system to improve the throughput of optical communications by exploiting the advantages of both communication systems [39–41]. In [42], the transmission over the hybrid FSO-mmW channel is considered to be more secure. In [43], authors developed a practical demonstration of hybrid transmission and claimed the overall performance with better connectivity and speed. In [3], the authors pragmatically claim that the individual optical channel can achieve 99.999% availability over a distance of 140m, while the hybrid system efficiently maximizes the connectivity distance. The aim of the hybrid FSO-RF system is to send the same signal copies concurrently over both channels and merge the received signals by exploiting the receive diversity combining technique. The combining is possible because both of the channels show compatible features to atmospheric and weather conditions whereas the radio channel is not prone to scintillation or snow and fog as the case of the FSO link, but rather to dense rain [44]. In [45,46], the researchers investigated that parallel optical-radio communication is a promising technology that exploits the complementary benefits of optical and radio link (i.e., robustness and high data rate). It is well known that although RF communications have a low risk of link failure, beam-directivity lags far behind that of FSO communications. Hence, most research on the hybrid FSO-RF systems assume a link-distance of no greater than a few kilometers to maximize the merits of additional RF links [47]. It is important that all the above-mentioned studies never focus on the optimization of the hybrid FSO-RF systems using the receive diversity combining techniques.

In the proposed method, the outage probability and system performance in terms of bit error rate (BER) have been optimized and analyzed. Free space communication system (FSCS) is deployed to significantly improve as well as reducing the total power consumption requirement under the induced atmospheric turbulence regime. It is likewise derived from the closed form of outage probability expression for the FSCS. In both RF and FSO links, in which SC and MRC combining techniques are implemented. In the FSO system, intensity modulation and direct detection (IM/DD) is employed. In FSCS, the advantages of combining both the FSO and RF links are the high data rate, and more secure and reliable links. On the other hand, FSCS can support the receiver in order to make a nice selection via the means of combining different copies of the original signal received from the channel and to enhance the system overall performance. Following are the main contributions of the proposed research;

- A novel hybrid system having single encoder and decoder is proposed. The benefits of proposing single encoder and decoder are as: cost effective system and no synchronization issue.

- To improve the performance of the proposed communication system, we develop a diversity algorithm, which exploits either of the diversity combining schemes (SC or MRC) and selects the best optimum.
- We develop a comparison between the single links (RF and FSO) and hybrid link and provide the simulation results.

2 Proposed System and Methods

2.1 Free Space Communication System (FSCS)

The proposed FSCS, where FSO and RF links deliver reliable transmission in outdoor wireless environments for real time mission and critical traffic. A typical block diagram of the proposed FSCS using the receive diversity combining techniques is shown in Fig. 1. Transmitter, receiver and channel are the major components of FSCS. FSCS includes parallel channels of FSO and RF with one encoder, which is used to reduce the implementation cost and minimize the computational complexity. The k-bits are encoded using the low-density parity check (LDPC) code into n bits code word. The code word bits are further divided into two streams where one stream (i.e., n_o bits) is sent through the optical channel and the other (i.e., n_r bits) through the RF channel. Then every bit stream is mapped to create corresponding RF and FSO symbols that are transmitted concurrently through the corresponding channel. Each symbol stream is then modulated using the individual channel modulator. The combined/hybrid symbols are transmitted through the single transmit antenna. At the receiver side, the combined signal is received by a number of receive antennas (i.e., $N_1, N_2, \ldots, N_t$). The receive diversity techniques (i.e., SC and MRC) are applied and the outage probability for each technique is analyzed. Analysis of SC and MRC are developed for the individual channel as well as for the FSCS and the overall performance of each system is compared.

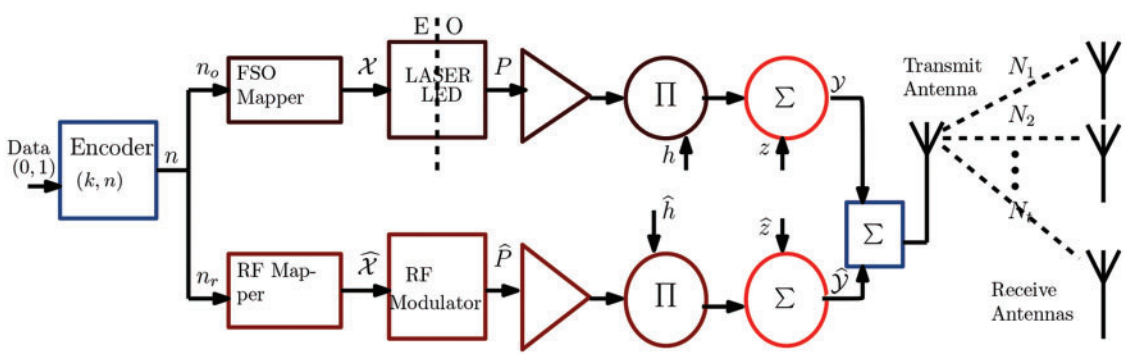

Figure 1: Block diagram of Free Space Communication System (FSCS)

2.2 Channel Model

In the FSCS system, FSO link is dynamic with instantaneous signal-to-noise ratio (SNR) on optical receiver γ_{FSO} that is the top definite threshold γ_{th}. Once it is going down the threshold level, the feedback signal is sent by the receiver to initiate RF in addition to FSO links concurrently, which transmits the equivalent data. At the receiving side, the signals received from each link are combined with the aid of a combiner. The receiver SNR designated with the aid of using γ_{snr}, so that it can be same to γ_{FSO} while $\gamma_{FSO} \geq \gamma_{th}$. On the alternative, while $\gamma_{FSO} < \gamma_{th}$, γ_{snr}could be the sum of γ_{FSO} and γ_{RF}. γ_{RF} is designated as an instantaneous SNR of RF link.

2.2.1 FSO Link Modelling

At the receiver, the optical received signal utilizing the IM/DD is modeled as Eq. (A.1) given in Appendix A. FSO Model. The model is dependent on the modulation process, in which the light radiation fluctuations are traversing a turbulent atmosphere, which is meant to include small and large scales effects correspondingly such as refraction and scattering. It characterizes the light irradiance, which is the product of two independent variables each with Gamma probability density function (PDF). The intensity (I) fluctuation of PDF is given as Eq. (1)

$$f(I) = \frac{2(\alpha\beta)^{(\alpha+\beta)/2}}{\Gamma(\alpha)\Gamma(\beta)} I^{\frac{(\alpha+\beta)}{2}-1} K_{(\alpha-\beta)}\left(2\sqrt{\alpha\beta I}\right), I \geq 0 \tag{1}$$

wherever $\Gamma(.)$ is that the gamma function. $K_n(.)$ is the improved 2nd order Bessel function, α and β, correspondingly, which constitute the powerful variety of small and large scales vertices of the scattering process. At receiver, the optical radiation is a plane wave, α and β that is characterize the irradiance fluctuation and are given in Eqs. (2) and (3)

$$\alpha = \left[\exp\left(\frac{0.49\sigma_R^2}{\left(1+1.11\sigma_R^{12/5}\right)^{7/6}}\right) - 1\right]^{-1} \tag{2}$$

$$\beta = \left[\exp\left(\frac{0.51\sigma_R^2}{\left(1+0.69\sigma_R^{12/5}\right)^{7/6}}\right) - 1\right]^{-1} \tag{3}$$

where σ_R^2 is the Rytov variance. The FSO link is related to I, which is received signal intensity and is related to SNR by $\gamma_{FSO} = \overline{\gamma}_{FSO} I^2$ given in Eq. (A.4), $E[.]$ is the expectation operator, the $E[I]$ normalized to unity, $\overline{\gamma}_{FSO}$ is the average electric SNR (see Eq. (A.5)). By using of power transformation, it is simple to calculate the PDF of γ_{FSO} as Eq. (4);

$$f_{\gamma_{FSO}}(\gamma_{FSO}) = \frac{(\alpha\beta)^{(\alpha+\beta)/2}}{\Gamma(\alpha)\Gamma(\beta)\overline{\gamma}_{FSO}^{\frac{(\alpha+\beta)}{4}}} \gamma_{FSO}^{\frac{(\alpha+\beta)}{4}-1} K_{(\alpha-\beta)}\left(2\sqrt{\alpha\beta\sqrt{\frac{\gamma_{FSO}}{\overline{\gamma}_{FSO}}}}\right), \gamma_{FSO} \geq 0 \tag{4}$$

To express $K_{(\alpha-\beta)}(.)$ in relations of Meijer G function and can be derived as Eq. (5) [26];

$$f_{\gamma_{FSO}}(\gamma_{FSO}) = \frac{\gamma_{FSO}^{-1}}{2\Gamma(\alpha)\Gamma(\beta)} G_{0,2}^{2,0}\left(\alpha\beta\sqrt{\frac{\gamma_{FSO}}{\overline{\gamma}_{FSO}}} - \alpha, \beta\right) \tag{5}$$

By using [48], the cumulative density function (CDF) of γ_{FSO} can be derived as Eq. (6);

$$F_{\gamma_{FSO}}(\gamma_{FSO}) = \frac{2^{\alpha+\beta-2}}{\pi\Gamma(\alpha)\Gamma(\beta)} \times G_{1,4}^{4,1}\left[\frac{(\alpha\beta)^2}{16\overline{\gamma}_{FSO}}\gamma_{FSO}\mathbf{1}\frac{\alpha}{2}, \frac{\alpha+1}{2}, \frac{\beta}{2}, \frac{\beta+1}{2}\right] \tag{6}$$

2.2.2 RF Link Modeling

Considering the RF power $\hat{P}$, the received RF signal is modeled by Eq. (B.1) given in Appendix B. RF Model. The RF link instantaneous received SNR γ_{RF} is defined by $\gamma_{RF} = \overline{\gamma}_{RF}\hat{h}^2$ by (see Eq. (B.4)) with $E[\hat{h}^2]$ normalized to unity. Average SNR $\overline{\gamma}_{RF}$ is defined in Eq. (B.3). The fading gain is displayed by Rice distribution (also known as Nakagami-n Model) and the PDF of γ_{RF} is given by Eq. (7) [49].

$$f_{\gamma_{RF}}\left(\gamma_{RF}\right)=\frac{K+1}{\overline{\gamma}_{RF}}\exp\left(-\left(K+1\right)\frac{\gamma_{RF}}{\overline{\gamma}_{RF}}-K\right)\times I_0\left(2\sqrt{K\left(K+1\right)\frac{\gamma_{RF}}{\overline{\gamma}_{RF}}}\right) \tag{7}$$

where K is that the Rician factor. It relies upon numerous link constraints, that is antenna height or link distance. Moreover, its CDF can be calculated as Eq. (8):

$$F_{\gamma_{RF}}\left(\gamma_{RF}\right)=1-Q_1\left(\sqrt{2K},\sqrt{2\left(K+1\right)\frac{\gamma_{RF}}{\overline{\gamma}_{RF}}}\right) \tag{8}$$

2.3 Diversity Combining Techniques

Diversity combining is suggested for mitigating the fading induced by the atmospheric turbulence. In the proposed system, SC and MRC diversity combining techniques are investigated and a comparison of each technique over the individual channel and the FSCS is developed to show the performance of each system under various conditions.

2.3.1 Selection Combining (SC)

SC is easy to deploy, in which a selection switch is employed and each branch is scanned overall SNR values. The receiving branch having the best instantaneous SNR is hooked up to the demodulator. The SNR output is calculated as Eq. (9);

$$\gamma_{SC}=\max(\gamma_{FSO},\gamma_{RF}) \tag{9}$$

The average BER of the SC can be obtained by Eq. (10);

$$p_{SC}=I\int_0^{\infty}Q\left(\sqrt{2\gamma_{SC}}B\right)f_{\gamma_{SC}}(\gamma_{SC})d\gamma_{SC} \tag{10}$$

where B is the bandwidth and $f_{\gamma_{SC}}$ (.) is the pdf of γ_{SC} as Eq. (11)

$$\overline{p}_{SC}(e)=\frac{I}{2\pi}\int_0^{\infty}exp\left(-\frac{x^2}{2}\right)F_{\gamma_{SC}}\left(\frac{x^2}{2B^2}\right)dx \tag{11}$$

The average BER of the receiver is approximated as Eq. (12);

$$\overline{p}_{SC}=\overline{p}_1\left(e\right)-J \tag{12}$$

wherever $\overline{p}_1\left(e\right)$ is that the FSO sub system BER estimated using the same procedure as in [50] and J is calculated as Eq. (13);

$$J=\frac{Iexp(-K)2^{\alpha+\beta-2}}{\pi^{\frac{3}{2}}\Gamma(\alpha)\Gamma(\beta)}\times\sum_{i=0}^{N}\sum_{j=0}^{i}\frac{K^i(K+1)^jq^{2j+1}}{\overline{\gamma}_{RF}^{j}B^{2j}2^ji!\,j!}\times G_{3,6}^{4,3}\left[\frac{(\alpha\beta q)^2}{16\overline{\gamma}_{FSO}B^2}\middle|\begin{matrix}\frac{1}{2},\mathbf{1},\frac{1}{2}-\boldsymbol{j}\\\frac{\alpha}{2},\frac{\alpha+1}{2},\frac{\beta}{2},\frac{\beta+1}{2},0,\frac{1}{2}\end{matrix}\right] \tag{13}$$

2.3.2 Maximal Ratio Combining (MRC)

No doubt, SC is simple to compute but it requires continuous scanning, and is not always a finest diversity combining technique. In MRC scheme, the received signals of each branch can be combined, wherein the SNR of the output signal is the addition of the SNR of each branch with a weighting coefficient and is determined as Eq. (14),

$$\gamma_{MRC}=\sqrt{\gamma_{FSO}}\frac{y}{\sigma_{n_{FSO}}}+\sqrt{\gamma_{RF}}\frac{\hat{y}}{\sigma_{n_{RF}}} \tag{14}$$

Now at the moment, the output SNR will be gained by Eq. (15)

$$\gamma_{MRC} = \gamma_{FSO} + \gamma_{RF} \tag{15}$$

In MRC scheme, average BER overall performance is expressed as Eq. (16)

$$p_{MRC} = I \int_0^\infty \int_0^\infty Q\left(\sqrt{2(\gamma_{FSO} + \gamma_{RF})B}\right) \times f_{\gamma_{FSO}}(\gamma_{FSO}) f_{\gamma_{RF}}(\gamma_{RF})\, d\gamma_{FSO} d\gamma_{RF} \tag{16}$$

Q-function approximation [48] is used to evaluate Eq. (16). Accordingly, the average BER is obtained by Eq. (17)

$$p_{MRC} \approx \frac{I}{12} M_1\left(B^2\right) M_2\left(B^2\right) + \frac{I}{4} M_1\left(\frac{4B^2}{3}\right) M_2\left(\frac{4B^2}{3}\right) \tag{17}$$

where $M_1(.)$ and $M_2(.)$ can be defined as Eqs. (18) and (19)

$$M_1(x) = \frac{2^{\alpha+\beta-2}}{\pi\Gamma(\alpha)\Gamma(\beta)} \times G_{1,4}^{4,1}\left[\frac{(\alpha\beta)^2}{16\overline{\gamma}_{FSO}x}\middle| \begin{matrix} \mathbf{1} \\ \frac{\alpha}{2}, \frac{\alpha+1}{2}, \frac{\beta}{2}, \frac{\beta+1}{2} \end{matrix}\right] \tag{18}$$

$$M_2(x) = \frac{K+1}{K+1+x\overline{\gamma}_{RF}} \exp\left(-\frac{Kx\overline{\gamma}_{RF}}{K+1+x\overline{\gamma}_{RF}}\right) \tag{19}$$

At the receiver, the average BER performance can be obtained by Eq. (20)

$$\overline{p}_{MRC} \approx \frac{I}{12} M\left(B^2\right) + \frac{I}{4} M\left(\frac{4B^2}{3}\right) \tag{20}$$

$M(.)$ is that the function described as Eq. (21)

$$M(x) = \frac{2^{\alpha+\beta-2}(K+1)\exp\left(-\frac{Kx\overline{\gamma}_{RF}}{K+1+x\overline{\gamma}_{RF}}\right)}{\pi\Gamma(\alpha)\Gamma(\beta)(K+1+x\overline{\gamma}_{RF})} \times G_{1,4}^{4,1}\left[\frac{(\alpha\beta)^2}{16\overline{\gamma}_{FSO}x}\middle| \begin{matrix} \mathbf{1} \\ \frac{\alpha}{2}, \frac{\alpha+1}{2}, \frac{\beta}{2}, \frac{\beta+1}{2} \end{matrix}\right] \tag{21}$$

2.3.3 Outage Probability

Outage is defined by the property that the instantaneous output SNR γ_{snr} is lower than the threshold γ_{th} (i.e., $\gamma_{snr} < \gamma_{th}$). The probability that the received SNR γ_{snr} is below the threshold γ_{th} may be obtained by the evaluating the CDF of γ_{snr} at γ_{th} as $P_{out} = F_{\gamma_{snr}}(\gamma_{th})$, Now, it is calculated as in Eqs. (22) and (23)

$$F_{\gamma_{snr}}(x) = p_r\left[\gamma_{FSO} \geq \gamma_{th}, \gamma_{FSO} < x\right] + p_r\left[\gamma_{FSO} < \gamma_{th}, \gamma_{FSO} + \gamma_{RF} < x\right] \tag{22}$$

$$= \begin{cases} F_1(x) & if x \leq \gamma_{th} \\ F_{\gamma_{FSO}}(x) - F_{\gamma_{FSO}}(\gamma_{th}) + F_2(x) & if x > \gamma_{th} \end{cases} \tag{23}$$

where $F_1(x)$ and $F_2(x)$ are defined as Eqs. (24) and (25)

$$F_1(x) = \int_0^x f_{\gamma_{FSO}+\gamma_{RF}}(\mathcal{Y})\, d\mathcal{Y} \tag{24}$$

$$F_2(x) = \int_0^x f_{\gamma_{FSO}}(\gamma_{FSO}) F_{\gamma_{RF}}(x - \gamma_{FSO})\, d\gamma_{FSO} \tag{25}$$

For the independent links, the $F_1(x)$ can be evaluated as Eq. (26)

$$f_{\gamma_{FSO}+\gamma_{RF}}(\mathcal{Y}) = \int_0^x f_{\gamma_{FSO}}(\gamma_{FSO}) f_{\gamma_{RF}}(\mathcal{Y} - \gamma_{FSO}) d\gamma_{FSO} \tag{26}$$

After substituting the values of $f_{\gamma_{FSO}}(\gamma_{FSO})$ and $f_{\gamma_{RF}}(\gamma_{RF})$ in Eq. (26) and applying the Binomial expansion [51], Eq. (26) can be estimated as Eq. (27),

$$f_{\gamma_{FSO}+\gamma_{RF}}(\mathcal{Y}) = \frac{2^{\alpha+\beta-2}(K+1)\exp\left(-\frac{Kx\overline{\gamma}_{RF}}{K+1+x\overline{\gamma}_{RF}}\right)}{\pi\Gamma(\alpha)\Gamma(\beta)(K+1+x\overline{\gamma}_{RF})} \times G_{1,4}^{4,1}\left[\frac{(\alpha\beta)^2}{16\overline{\gamma}_{FSO}}\gamma_{FSO}\,\middle|\,\begin{matrix}\boldsymbol{K_1}\\ K_2\end{matrix}\right] \tag{27}$$

The combining techniques is employed over the proposed algorithm and error performance results are better.

Algorithm

1: Procedure Initialization (define P_i and Encoder with (k, n)).

2: Define bits with two streams n_o for optical n_r for RF. Every bit stream is mapped to create RF and FSO symbols i.e., $\hat{\mathcal{X}}$ and $\mathcal{X}$, which is transmitted according to the channel.

3: Each symbol is modulated according to their channel modulator i.e., P is optical power and $\hat{P}$ is RF power.

4: The combined symbols are transmitted through single transmit antenna.

5: At the receiver side, the combined signal is received by number of receive antennas i.e., $(N_1, N_2, \ldots, N_t)$.

6: The receive diversity techniques are applied that is

a. For selection combining (SC) is evaluated as;

$$\overline{p}_{SC} = \overline{p}_1(e) - J$$

$$J = \frac{I exp(-K) 2^{\alpha+\beta-2}}{\pi^{\frac{3}{2}}\Gamma(\alpha)\Gamma(\beta)} \times \sum_{i=0}^{N}\sum_{j=0}^{i} \frac{K^i (K+1)^j q^{2j+1}}{\overline{\gamma}_{RF}^{j} B^{2j} 2^j i!\, j!} \times G_{3,6}^{4,3}\left[\frac{(\alpha\beta q)^2}{16\overline{\gamma}_{FSO}B^2}\,\middle|\,\begin{matrix}\boldsymbol{\frac{1}{2}, 1, \frac{1}{2} - j}\\ \frac{\alpha}{2}, \frac{\alpha+1}{2}, \frac{\beta}{2}, \frac{\beta+1}{2}, 0, \frac{1}{2}\end{matrix}\right]$$

b. For maximal ratio combining (MRC) is evaluated as;

$$\overline{p}_{MRC} \approx \frac{I}{12} M\left(B^2\right) + \frac{I}{4} M\left(\frac{4B^2}{3}\right)$$

$$M(x) = \frac{2^{\alpha+\beta-2}(K+1)\exp\left(-\frac{Kx\overline{\gamma}_{RF}}{K+1+x\overline{\gamma}_{RF}}\right)}{\pi\Gamma(\alpha)\Gamma(\beta)\left(K+1+x\overline{\gamma}_{RF}\right)} \times G_{1,4}^{4,1}\left[\frac{(\alpha\beta)^2}{16\overline{\gamma}_{FSO}x}\,\middle|\,\begin{matrix}\boldsymbol{1}\\ \frac{\alpha}{2}, \frac{\alpha+1}{2}, \frac{\beta}{2}, \frac{\beta+1}{2}\end{matrix}\right]$$

c. For outage probability both system is combined and is analyzed as;

(Continued)

Algorithm Continued

$$f_{\gamma_{FSO}+\gamma_{RF}}(\mathcal{Y}) = \frac{2^{\alpha+\beta-2}(K+1)\exp\left(-\frac{Kx\overline{\gamma}_{RF}}{K+1+x\overline{\gamma}_{RF}}\right)}{\pi\Gamma(\alpha)\Gamma(\beta)\left(K+1+x\overline{\gamma}_{RF}\right)} \times G_{1,4}^{4,1}\left[\frac{(\alpha\beta)^2}{16\overline{\gamma}_{FSO}}\gamma_{FSO}\middle| \begin{matrix} \boldsymbol{K}_1 \\ K_2 \end{matrix}\right]$$

7: Finally, we get average bit error rate (BER) evaluation exploiting the SC and MRC techniques over a distinct number of receive antennas. Also, comparison of SC and MRC technique evaluating the outage probability for individual channels, RF, FSO and FSCS.

8: The criteria are achieved by applying the above techniques and overall performance is better.

3 Results and Discussion

The performance of the presented FSCS system and the individual channels (i.e., RF and FSO) is evaluated assuming SC and MRC combining techniques under strong turbulence channel conditions. For the simulation purpose, we use MATLAB. For the strong atmospheric turbulence, we assume $\alpha = 2.064, \beta = 1.342$ and $C_n^2 = 1.8 \times 10^{-14} m^{-2/3}$. Both the combining schemes are analyzed in terms of average BER and outage probability by considering a distinct number of receive antennas. The average BER is evaluated considering both the combining schemes (SC and MRC) for the FSCS system and the results are presented in Figs. 2 and 3 respectively. Fig. 2 shows the average BER estimated using the SC technique for a distinct number of antennas. It can be observed that the improvement of using 6 receiving antennas with respect to the 2 receiving antenna is about $10dB$ at $BER = 10^{-4}$.

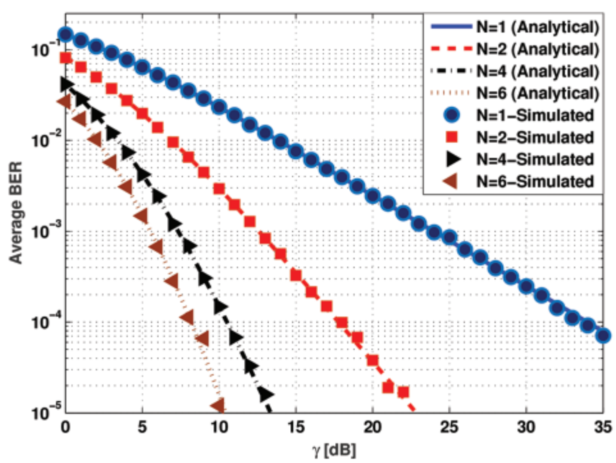

Figure 2: Average BER evaluation exploiting the SC technique over a distinct number of receive antennas

The MRC combining technique is evaluated and the simulation results of average BER are plotted exploiting the distinctive number of antennas in Fig. 3. It can be observed that the improvement of using 6 receiving antennas with respect to 2 receiving antenna is about $12dB$ at $BER = 10^{-4}$.

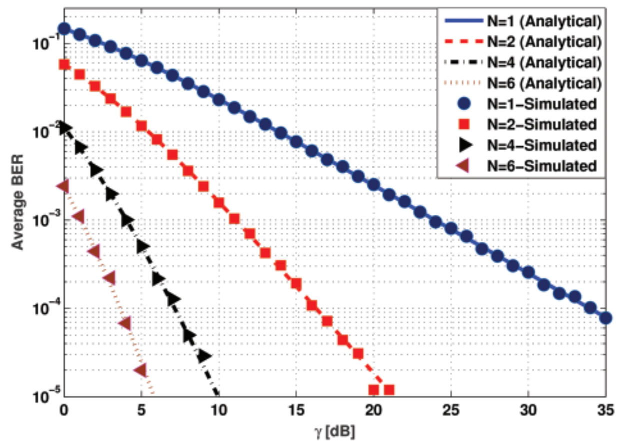

Figure 3: Evaluation of average BER exploiting the MRC technique using distinct number of receive antennas

In Fig. 4, the outage probability is evaluated employing both of the SC and MRC combining techniques and the results are compared for the individual channel (i.e., RF and FSO) as well as for the FSCS respectively. The simulation is performed for a fixed number of receive antenna (i.e., $N = 3$). It is clearly seen that the MRC combining techniques outperforms the SC combining technique with the price of extra computational complexity. On the other hand, it is also observed that the FSCS system outperforms the individual transmission channels (i.e., FSO and RF).

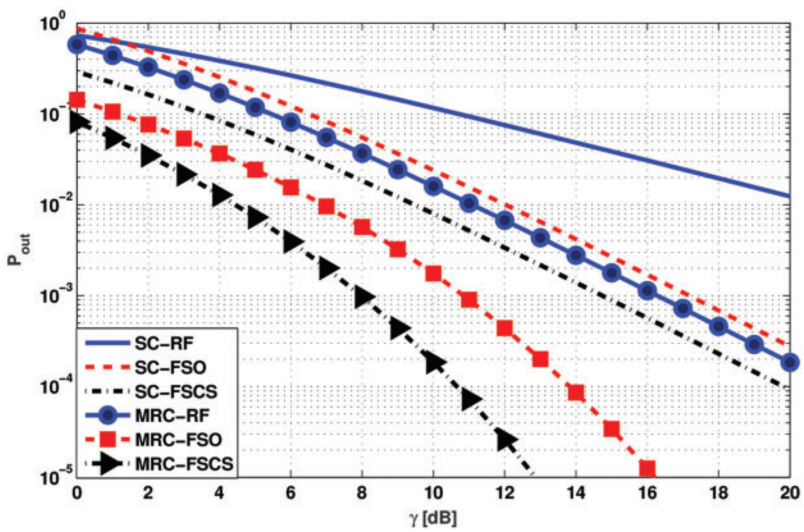

Figure 4: Comparison of SC and MRC technique evaluating the outage probability for individual channels (i.e., RF and FSO) and the FSCS, when N = 3

In Fig. 5, the outage probability of the FSCS employing the MRC technique is evaluated and the simulation results are plotted for a distinctive number of receive antennas. The SNR required to accomplish the aim of outage probability of $P_{out} = 10^{-5}$, is approximately of 3 dB difference among the instances $N = 4$ and $N = 6$. Therefore, the totaling of the most effective one receiver reduces the power consumption. This shows that the proposed system is suitable for the optimum reduced power consumption in various situations, which is the most attractive assignment in a communication system. It is likewise noticed that further diversity gain can also be achieved by utilizing a wide variety of receive apertures, which is anticipated from the results at the high SNR regime.

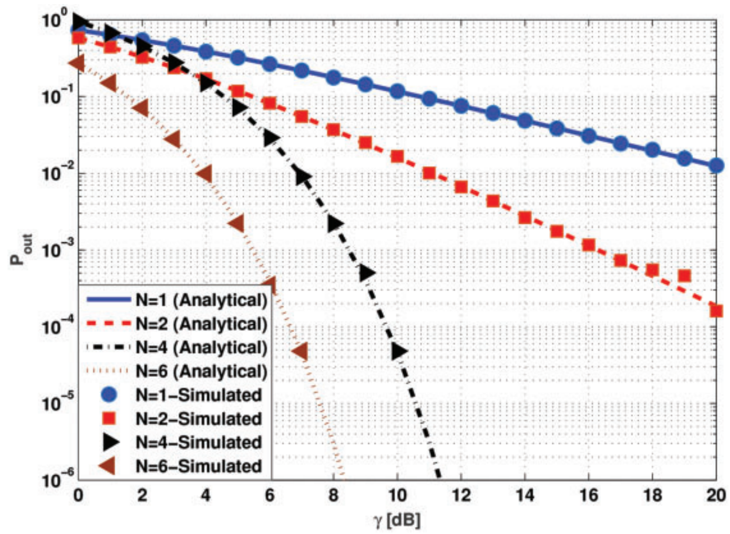

Figure 5: Evaluating the outage probability of the FSCS system exploiting different number of receive antennas and MRC combining technique

In this paper, we have compared the performance of FSO and RF systems with receive diversity compared with proposed FSCS. Outage probability of FSO and RF systems is compared with proposed FSCS in terms of SNR as shown in Fig. 6. At low outage probability of FSO is less than RF, which is almost equal with proposed FSCS with the increase of γ and its performance degrades. According to these simulations, FSCS system performance is better than for the other two systems.

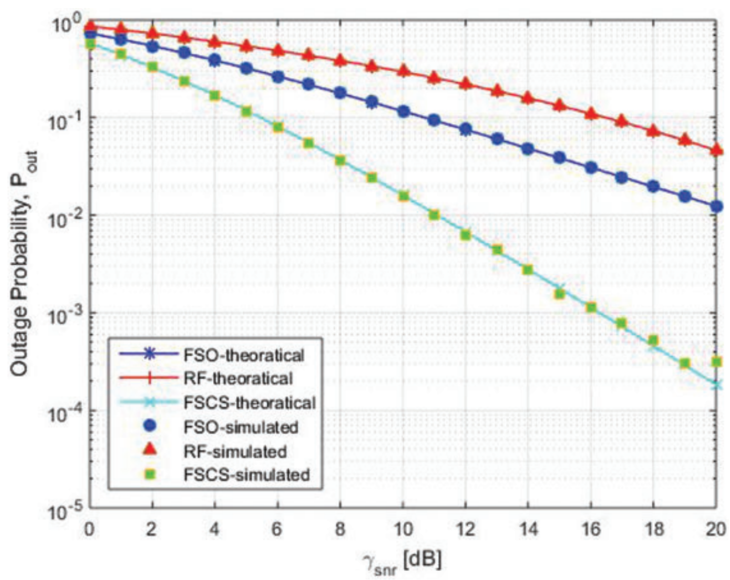

Figure 6: Comparison FSO, RF and FSCS

4 Conclusion

In this paper, the FSCS system is proposed and different combining techniques, i.e., SC and MRC are developed considering the receive diversity. The outage probability and the average BER metrics are evaluated. Closed form expressions for the outage probability and BER for both the SC and MRC are derived. Simulation is performed over a distinct number of receive antennas employing the FSO, RF and FSCS systems. The proposed system FSCS outperforms the individual FSO and RF communication systems under strong atmospheric turbulence in terms of power gains for a fixed number of antennas as is shown in simulation results. From the simulation results, it is seen that using MRC, FSCS system performs well as compared to SC and giving a power gain of 2 dB over distinct receive antennas. Further from the simulation results, it is also seen that the FSCS provides a gain of approximately 3 dB by exploiting 6 antennas as compared to 4 antennas.

The system model developed in this paper can be further investigated. We also believe that the proposed research works on the adaptive FSCS, which provides the better initialization for future research in terms of adaptivity and flexibility. For example, we apply our system model on MIMO, which would be interesting to investigate as well as consider the RF channel as a Rician fading channel and see its effects on the system.

Acknowledgement: The authors would like to thank Dr. Tausif Zahid and Dr. Qasim Awais for their thorough discussion and helping in completing the research work.

Funding Statement: The authors received no specific funding for this study.

Conflicts of Interest: The authors declare that they have no conflicts of interest to report regarding the present study.

References

[1] M. A. Khalighi and M. Uysal, "Survey on free space optical communication: A communication theory Perspective," *IEEE Communication Survey Tutorials*, vol. 16, no. 4, pp. 2231–2258, 2014.
[2] M. N. Khan, H. Kashif and A. Rafay, "Performance and optimization of hybrid FSO/RF communication system in varying weather," *Photonic Networking Communication*, vol. 2020, no. 1, pp. 1–10, 2021.
[3] T. Rakia, H. C. Yang, M. S. Alouini and F. Gebali, "Outage analysis of practical FSO/RF hybrid system with adaptive combining," *IEEE Communication Letters*, vol. 19, no. 8, pp. 1366–1369, 2015.
[4] Q. Fan, G. Zhou, T. Gui, C. Lu and A. Lau, "Advancing theoretical understanding and practical performance of signal processing for nonlinear optical communications through machine learning," *Nature Communication*, vol. 11, no. 1, pp. 1–11, 2020.
[5] A. Lobato, F. Ferreira, B. Inan, S. Adhikari, M. Kuschnerov *et al.,* "Maximum-likelihood detection in few-mode fiber transmission with mode-dependent loss," *IEEE Photonics Technology Letter*, vol. 25, no. 12, pp. 1095–1098, 2013.
[6] J. Anguita, M. Neifeld and B. Vasic, "Turbulence-induced channel crosstalk in an orbital angular momentum-multiplexed free-space optical link," *Applied Optics*, vol. 47, no. 13, pp. 2414–2429, 2008.
[7] G. Xie, L. Li, Y. Ren, H. Huang, Y. Yan *et al.,* "Performance metrics and design considerations for a free-space optical orbital-angular-momentum-multiplexed communication link," *Optica*, vol. 2, no. 4, pp. 357–365, 2015.
[8] K. Fontaine, R. Ryf, H. Chen, D. T. Neilson, K. Kim *et al.,* "Longevity defined as top 10% survivors and beyond is transmitted as a quantitative genetic trait," *Nature Communications*, vol. 10, no. 1, pp. 35, 2019.

[9] H. Song, H. Song, R. Zhang, K. Manukyan, L. Li *et al.,* “Experimental mitigation of atmospheric turbulence effect using pre-signal combining for uni- and bi-directional free-space optical links with two 100-Gbit/s OAM-multiplexed channels,” *Journal of Lightwave Technology*, vol. 38, no. 1, pp. 82–89, 2020.

[10] P. Freire, J. Prilepsky, Y. Osadchuk, S. Turitsyn and V. Aref, “Neural networks based post-equalization in coherent optical systems: Regression versus classification,” *arXiv preprint arXiv:2109.13843*, vol. 2, pp. 1–9, 2021.

[11] X. Liu, H. Lun, M. Fu, Y. Fan, L. Yi *et al.,* “AI-based modeling and monitoring techniques for future intelligent elastic optical networks,” *Applied Science*, vol. 10, no. 1, pp. 363, 2020.

[12] B. Yin, S. W. Zhou, S. W. Zhang, K. Gu and F. Yu, “On efficient processing of continuous reverse skyline queries in wireless sensor networks,” *KSII Transactions on Internet and Information Systems*, vol. 11, no. 4, pp. 1931–1953, 2017.

[13] J. M. Zhang, K. Yang, L. Y. Xiang, Y. S. Luo, B. Xiong *et al.,* “A self-adaptive regression-based multivariate data compression scheme with error bound in wireless sensor networks,” *International Journal of Distributed Sensor Networks*, vol. 9, no. 3, pp. 913497, 2013.

[14] J. Wang, C. Ju, Y. Gao, A. K. Sangaiah and G. J. Kim, “A PSO based energy efficient coverage control algorithm for wireless sensor networks,” *Computers Materials & Continua*, vol. 56, no. 3, pp. 433–446, 2018.

[15] J. Wang, X. J. Gu, W. Liu, A. K. Sangaiah and H. J. Kim, “An empower hamilton loop based data collection algorithm with mobile agent for WSNs,” *Human-centric Computing and Information Sciences*, vol. 9, no. 1, pp. 1–14, 2019.

[16] J. Wang, Y. Gao, C. Zhou, S. Sherratt and L. Wang, “Optimal coverage multi-path scheduling scheme with multiple mobile sinks for WSNs,” *Computers, Materials & Continua*, vol. 62, no. 2, pp. 695–711, 2020.

[17] J. Wang, Y. Gao, W. Liu, W. Wu and S. J. Lim, “An asynchronous clustering and mobile data gathering schema based on timer mechanism in wireless sensor networks,” *Computers, Materials & Continua*, vol. 58, no. 3, pp. 711–725, 2019.

[18] J. Wang, Y. Gao, X. Yin, F. Li and H. J. Kim, “An enhanced PEGASIS algorithm with mobile sink support for wireless sensor networks,” *Wireless Communications and Mobile Computing*, vol. 2018, pp. 1–9, 2018.

[19] Q. Tang, K. Yang, P. Li, J. M. Zhang, Y. S. Luo *et al.,* “An energy efficient MCDS construction algorithm for wireless sensor networks,” *EURASIP Journal on Wireless Communications and Networking*, vol. 2012, no. 1, pp. 102, 2012.

[20] Z. Liao, J. Wang, S. Zhang, J. Cao and G. Min, “Minimizing movement for target coverage and network connectivity in mobile sensor networks,” *IEEE Transactions on Parallel and Distributed Systems*, vol. 26, no. 7, pp. 1971–1983, 2014.

[21] M. Portnoi, P. A. Haigh, T. J. Macdonald, F. Ambroz, I. P. Parkin *et al.,* “Bandwidth limits of luminescent solar concentrators as detectors in free-space optical communication systems,” *Light: Science & Applications*, vol. 10, no. 1, pp. 1–12, 2021.

[22] H. Huang, G. Xie, Y. Yan, N. Ahmed, Y. Ren *et al.,* “100 Tbit/s free-space data link enabled by three-dimensional multiplexing of orbital angular momentum, polarization, and wavelength,” *Optics Letters*, vol. 39, no. 2, pp. 197–200, 2014.

[23] A. Willner and C. Liu, “Perspective on using multiple orbital-angular-momentum beams for enhanced capacity in free-space optical communication links,” *Nanophotonics*, vol. 10, no. 1, pp. 225–233, 2021.

[24] T. Xu, N. A. Shevchenko, Y. Zhang, C. Jin, J. Zhao *et al.,* “Information rates in kerr nonlinearity limited optical fibre communication systems,” *Optics Express*, vol. 29, no. 11, pp. 17428–17439, 2021.

[25] Z. Yang, W. Yu, G. Peng, Y. Liu and L. Zhang, “Recent progress on novel DSP techniques for mode division multiplexing systems: A Review,” *Applied Science*, vol. 11, no. 4, pp. 1363, 2021.

[26] H. Kashif, M. N. Khan and A. Altalbe, “Hybrid optical-radio transmission system link quality: link budget analysis,” *IEEE Access*, vol. 8, pp. 65983–65992, 2020.

[27] M. Uysal, J. Li and M. Yu, “Error rate performance analysis of coded free-space optical links over gamma-gamma atmospheric turbulence channels,” *IEEE Transaction on Wireless Communication*, vol. 5, no. 6, pp. 1229–1233, 2006.

[28] X. Zhu, J. Kahn and J. Wang, "Mitigation of turbulence-induced scintillation noise in free-space optical links using temporal-domain detection techniques," *IEEE Photonics Technology Letters*, vol. 15, no. 4, pp. 623–625, 2003.
[29] S. Navidpour, M. Uysal and M. Kavehrad, "BER performance of free-space optical transmission with spatial diversity," *IEEE Transaction on Wireless Communication*, vol. 6, no. 8, pp. 2813–2819, 2007.
[30] E. J. Lee and V. Chan, "Diversity coherent receivers for optical communication over the clear turbulent atmosphere," in *IEEE Int. Conf. on Communications*, Glasgow, UK, pp. 2485–2492, 2007.
[31] E. J. Lee and V. Chan, "Diversity coherent and incoherent receivers for free-space optical communication in the presence and absence of interference," *Journal of Optical Communications and Networking*, vol. 1, no. 5, pp. 463–483, 2009.
[32] N. Letzepis and A. G. Fabregas, "Outage probability of the gaussian mimo free-space optical channel with PPM," *IEEE Transactions on Communications*, vol. 57, no. 12, pp. 3682–3690, 2009.
[33] F. Xu, M. A. Khalighi, P. Causse and S. Bourennane, "Channel coding and time-diversity for optical wireless links," *Optics Express*, vol. 17, no. 2, pp. 872–887, 2009.
[34] W. Popoola and Z. Ghassemlooy, "BPSK subcarrier intensity modulated free-space optical communications in atmospheric turbulence," *Journal of Lightwave technology*, vol. 27, no. 8, pp. 967–973, 2009.
[35] H. Manor and S. Arnon, "Performance of an optical wireless communication system as a function of wavelength," *Applied Optics*, vol. 42, no. 21, pp. 4285–4290, 2003.
[36] E. Lee and V. W. Chan, "Part 1: Optical communication over the clear turbulent atmospheric channel using diversity," *IEEE Journal on Selected Areas in Communications*, vol. 22, no. 9, pp. 1896–1906, 2004.
[37] M. A. Amirabadi, "New expression on the performance of a novel multi-hop relay-assisted hybrid FSO/RF communication system with receive diversity," *arXiv preprint arXiv:1806.02269*, vol. 2, pp. 1–8, 2018.
[38] H. Wang, L. Xu and X. Wang, "Outage probability performance prediction for mobile cooperative communication networks based on artificial neural network," *Sensors*, vol. 19, no. 21, pp. 4789, 2019.
[39] S. Ghoname, H. A. Fayed, A. A. Aziz and M. H. Aly, "Performance evaluation of an adaptive hybrid FSO/RF communication system: Impact of weather attenuation," *Iranian Journal of Science and Technology, Transactions of Electrical Engineering*, vol. 44, no. 1, pp. 119–128, 2020.
[40] N. Vishwakarma and S. Ramabadran, "Performance analysis of hybrid FSO/RF communication over generalized fading models," *Optics Communication*, vol. 487, no. 4, pp. 126796, 2021.
[41] H. Liang, Y. Li, M. Miao, C. Gao and X. Li, "Analysis of selection combining hybrid FSO/RF systems considering physical layer security and interference," *Optics Communication*, vol. 497, no. 11, pp. 127146, 2021.
[42] S. Song, Y. Liu, T. Xu, S. Liao and L. Guo, "Channel prediction for intelligent fso transmission system," *Optics Express*, vol. 29, no. 17, pp. 27882–27899, 2021.
[43] M. Amirabadi and V. Vakili, "A novel hybrid FSO/RF communication system with receive diversity," *Optik*, vol. 184, no. June 6, pp. 293–298, 2018.
[44] C. Wei and Z. Zhang, "Analysis of dual-hop AF relay systems in mixed RF and FSO links," *arXiv preprint arXiv:1711.09520*, vol. 1, pp. 1–4, 2017.
[45] M. Kafafy, Y. Fahmy, M. M. Khairy and M. Abdallah, "Secure backhauling over adaptive parallel mmwave/FSO link," in *IEEE Int. Conf. on Communications Workshops*, Dublin, Ireland, pp. 1–6, 2020.
[46] M. Amirabadi and V. Vakili, "On the performance of a novel multi-hop relay-assisted hybrid FSO/RF communication system with receive diversity," *Optik*, vol. 226, no. 2, pp. 165883, 2021.
[47] M. Siddharth, S. Shah, N. Vishwakarma and S. Ramabadran, "Performance analysis of adaptive combining based hybrid FSO/RF terrestrial communication," *IET Communication*, vol. 14, no. 22, pp. 4057–4068, 2021.
[48] M. Chiani, D. Dardari and M. K. Simon, "New exponential bounds and approximations for the computation of error probability in fading channels," *IEEE Transaction on Wireless Communication*, vol. 2, no. 4, pp. 840–845, 2003.
[49] M. K. Simon and M. S. Alouini, "Digital communications over fading channels," *IEEE Transactions on Information Theory*, vol. 54, no. 7, pp. 3369–3370, 2005.

[50] F. Zhang, T. Jing, Y. Huo and K. Jiang, "Outage probability minimization for energy harvesting cognitive radio sensor networks," *Sensors*, vol. 17, no. 2, pp. 224, 2017.
[51] I. Gradshteyn and I. Ryzhik, *Table of integrals, series, and products*. Academic Press, USA, 2014.
[52] S. Bloom and S. Hartley, *The last mile solution: Hybrid FSO radio*. Whitepaper, AirFiber Inc, Seattle WA, USA, pp. 1–20, 2002.
[53] B. He and R. Schober, "Bit-interleaved coded modulation for hybrid RF/FSO systems," *IEEE Transaction on Communication*, vol. 57, no. 12, pp. 3753–3763, 2009.

Appendix A. FSO Model

Considering an optical power P, the received FSO signal ($\mathcal{Y}$) employing the IM/DD mapping scheme is given as Eq. (A.1),

$$\mathcal{Y}(t) = T\mathcal{X}(t) + z(t) \tag{A.1}$$

where $\mathcal{X}$ is the optical symbols assuming the On-Off Keying (OOK) modulation, $T = \eta Ph$, η represents that the conversion detectors efficiency, P is that the optical power and h is that the fading gain (channel) and $z(t)$ is that the noise, which is signal independent additive white Gaussian noise with zero-mean and variance $\sigma^2_{n_{FSO}}$. We expect the operation with the excessive SNR regime, in which ambient light predominates due to shot noise. Consequently, the Gaussian noise model is used as an excellent calculation for detection. After the demodulation of photo-detector electric output, the DC bias is filtered out and the received discrete-time equivalent signal output from the of the FSO receiver is given as Eq. (A.2),

$$\mathcal{Y}(t) = \mu\eta\sqrt{\frac{E_s}{2}}Phg\mathcal{X}(t) + z(t) \tag{A.2}$$

where g denote FSO link average gain and E_s denotes the symbol energy, μ is that the modulation index, which lies between the $0 < \mu < 1$. Supposing ideal alignment among the transmitter and receiver, g can be defined as Eq. (A.3), [52].

$$g = \frac{\pi D^2}{4(\theta L)^2}\exp(-h\zeta l) \tag{A.3}$$

where ζ is that the climate dependent attenuation coefficient approximately 1 per km, θ is represents the divergence of the transmit beam, D is that the diameter of receiver aperture and L is that the distance link. From Eq. (A.2), instantaneous electric SNR of the FSO receiver can be defined as Eq. (A.4),

$$\gamma_{FSO} = \overline{\gamma}_{FSO}h^2 \tag{A.4}$$

where $\overline{\gamma}_{FSO}$ is the electric average SNR and is given as Eq. (A.5),

$$\overline{\gamma}_{FSO} = \frac{\mu^2\eta^2P^2E_sg^2}{\sigma^2_{n_{FSO}}} \tag{A.5}$$

Appendix B. RF Model

Consider the RF power $\hat{P}$, the received RF signal is expressed by Eq. (B.1),

$$\hat{\mathcal{Y}}(t) = T\hat{\mathcal{X}}(t) + \hat{z}(t) \tag{B.1}$$

where $\hat{\mathcal{Y}}(t)$ represents the received RF signal $\hat{T} = \hat{P}\hat{h}$, $\hat{\mathcal{X}}$, where $\hat{\mathcal{X}}$denotes the RF symbols, transmitted using binary phase shift keying (BPSK), $\hat{h}$ represent RF channel fading gain. $\hat{z}(t)$ denotes a random value of additive white Gaussian noise (AWGN). Now, it shows as in Eq. (B.2)

$$\hat{\mathcal{Y}}(t) = \sqrt{\hat{P}}\sqrt{\hat{g}}\hat{h}\sqrt{\hat{E}_s}\hat{\mathcal{X}}(t) + \hat{z}(t) \tag{B.2}$$

where $\hat{g}$ is that the RF link average power gain and $\hat{E}_s$ is the RF symbol energy. RF link average power gain is expressed as Eq. (B.3), [53]

$$\hat{g}\,[dB] = G_t - G_r - 20log_{10}\left(\frac{4\pi L}{\lambda}\right) - \alpha_{absorption}L - \alpha_{rain} \tag{B.3}$$

where G_t and G_r denote the gains of transmit and receive antennas correspondingly. λ is that RF system wavelength, α_{rain} and $\alpha_{absorption}$are the weather attenuations [30]. The RF link instantaneous SNR is well described as Eq. (B.4),

$$\gamma_{RF} = \overline{\gamma}_{RF}\hat{h}^2 \tag{B.4}$$

where $\overline{\gamma}_{RF}$ representing the average SNR and is given by Eq. (B.5),

$$\overline{\gamma}_{RF} = \frac{\hat{P}^2 E_s \hat{g}^2}{\sigma^2_{n_{RF}}} \tag{B.5}$$